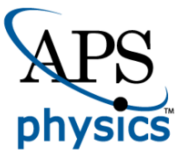

One-dimensional Bose gas dynamics: Breather relaxation

Bogdan Opanchuk and Peter D. Drummond

Phys. Rev. A **96**, 053628 — Published 27 November 2017

DOI: 10.1103/PhysRevA.96.053628

One-dimensional Bose gas dynamics: breather relaxation

Bogdan Opanchuk and Peter D. Drummond
Centre for Quantum and Optical Science, Swinburne University of Technology, Melbourne 3122, Australia

One-dimensional Bose gases are a useful testing-ground for quantum dynamics in many-body theory. They allow experimental tests of many-body theory predictions in an exponentially complex quantum system. Here we calculate the dynamics of a higher-order soliton in the mesoscopic case of $N = 10^3 - 10^4$ particles, giving predictions for quantum soliton breather relaxation. These quantum predictions use a truncated Wigner approximation, which is a $1/N$ expansion, in a regime where other exactly known predictions are recovered to high accuracy. Such dynamical calculations are testable in forthcoming BEC experiments.

Equilibrium calculations have been the staple diet of quantum many body theorists for many years. Yet this only scratches the surface. The dynamical properties of many-body quantum systems have enormous inherent complexity. Time evolution traces out a far larger set of quantum states than a ground state can.

Just as classical dynamics encompasses more interesting phenomena than static equilibria, the study of quantum systems far from equilibrium is therefore of much general interest. Quantum technologies at ultra-low temperatures can be manipulated in nearly lossless environments, allowing theoretical predictions to be tested.

In this Letter, we investigate one such quantum system: the one-dimensional attractive Bose gas. Ultracold atomic physics experiments can now investigate the quantum dynamics of these systems in mesoscopic regimes. Neither few-body physics nor the classical limit are dominant, leading to novel behaviour.

Experiments in photonics on these systems have investigated macroscopic, million-particle regimes, where squeezing and entanglement occur [1–4]. While providing important first-principles tests, these experiments did not yield large quantitative changes. Here, we investigate mesoscopic, thousand-particle regimes accessible in cold-atom experiments, where quantum changes are as large as the initial field itself, and do not occur classically.

The 1D Bose gas, with its conservation laws [5] and exact static solutions [6, 7] is an excellent testing ground for many-body theory. Second-order correlations in thermal equilibrium with repulsive interactions have been predicted [8–11] and verified experimentally [12, 13]. There is evidence of metastable steady-states with no Gibbs equilibrium [14, 15]. Attractive matter-wave solitons have been experimentally observed [16–21].

We show that higher-order matter-wave solitons are quantum-mechanically unstable. Fragmentation and damping of breathing oscillations [22, 23] are predicted to be very strong, even at particle numbers as large as $N = 1000$. These calculations use the truncated Wigner approximation, which is a $1/N$ expansion [24–26]. This is a regime accessible to BEC experiments [21, 23, 27], where closely related modulational instabilities have been experimentally observed.

An earlier calculation [28] used a variational approach with two spatial modes, predicting a sudden break-up into a pair of equal size fragments. This calculation was recently shown to be non-converged, violating known quantum center-of-mass (COM) expansion physics [29]. Our results throw new light on this analysis. The predictions obtained here are completely different, with a gradual fragmentation and many possible final states.

Fragmentation causes a relaxation in the oscillation of classical 'breathers' that we predict to happen gradually, without the abrupt changes after a short evolution time found by variational methods [28]. This is because the number of dissociation channels available is larger than the number of modes used in such calculations.

The oscillation decay found here is also different to that predicted at very small particle number either from DMRG methods [22], or using an exact analysis [23]. However, this difference is consistent with the scaling we find with N: fragmentation and breather relaxation are reduced as N increases.

Our calculations preserve all local conservation laws and (nearly) exact COM dynamics [30], giving results that are both quantitatively and qualitatively different to either classical predictions or to variational studies. This presents a novel opportunity for experimental tests of quantum dynamical predictions in regimes where no exact results are known.

In one dimensional optical or atomic waveguides, a similar Hamiltonian applies to either massive atomic Bose-Einstein condensate (BEC) experiments or to photonic experiments, where dispersion gives rise to an effective mass. If the bosons are confined to a single transverse mode, one obtains an 1D Bose gas theory, valid for low energies:

$$\hat{H}_{1\mathrm{D}} = \int \hat{\Psi}^\dagger_{1\mathrm{D}} H_1 \hat{\Psi}_{1\mathrm{D}} dr_3 + \frac{g_{1\mathrm{D}}}{2} \int \left(\hat{\Psi}^\dagger_{1\mathrm{D}}\right)^2 \hat{\Psi}^2_{1\mathrm{D}} dr_3 \,. \tag{1}$$

Here, $\boldsymbol{r}$ is the spatial coordinate, with a one-dimensional confinement so the dynamics occur in the r_3 direction. The mass is m, and for an atomic Bose gas in a parabolic

trap one has:

$$H_1 = -\hbar^2\partial_3^2/2m + m\omega_3^2 r_3^2/2$$
$$g_{1D} = 2\hbar\omega_\perp a\,, \tag{2}$$

where a is the three-dimensional S-wave scattering length, and the effective transverse trapping frequency of: $\omega_\perp = \sqrt{\omega_1\omega_2}$. If the system is photonic or polaritonic, as in a fibre optical experiment [2, 25, 31], the relevant parameters come from the dispersion and optical nonlinearity properties of the fiber.

This can be transformed to dimensionless form by choosing a length scale r_0 and time scale t_0 such that $r_0^2 = \hbar t_0/2m$. Distance is scaled too, so that $z = r_3/r_0$, and time is scaled to give a dimensionless time $\tau = t/t_0$. The resulting Hamiltonian, in the form introduced by Lieb and Liniger [6], with a dimensionless wave-function $\hat{\psi} = \sqrt{r_0}\hat{\Psi}_{1D}$, is:

$$\hat{H} = \int dz \left[\hat{\psi}^\dagger_{,z}(z)\hat{\psi}_{,z}(z) + C\left(\hat{\psi}^\dagger(z)\right)^2\hat{\psi}^2(z)\right]. \tag{3}$$

We use a subscript to indicate a derivative, so that:

$$\hat{\psi}_{,z}(z) \equiv \partial_z\hat{\psi}(z) \equiv \frac{\partial}{\partial z}\hat{\psi}(z)\,. \tag{4}$$

The following relationships exist between the physical and dimensionless units in the case of a trapped Bose-Einstein condensate [10, 32]: $\hat{H} = \hat{H}_1/E_0$, $E_0 = \hbar/t_0 = \hbar^2/2mr_0^2$ and $C = mg_{1D}r_0/\hbar^2 = 2m\omega_\perp r_0 a/\hbar$. A convenient procedure for solitons is to simply define r_0 as the characteristic initial dimension, so that C is of the order of the inverse particle number N.

The corresponding dynamical equation is known as the one-dimensional quantum nonlinear Schrodinger equation. It also describes quantum photonic propagation in one-dimensional optical fibers [33], under similar conditions of tight transverse confinement. Thus, an almost identical picture holds for 1D photonic systems [31, 33], except for additional Raman-Brillouin coupling to phonons, owing to the use of dielectric waveguides [34, 35]. This earlier work used phase-space techniques that originate in the work of Wigner [36] and Glauber [37]. Such predictions have been experimentally verified [1, 31, 38]. In both the photonic and atomic experiments, there are additional dissipative couplings due to linear and nonlinear losses and phase noise, leading to additional corrections. For simplicity, dissipation is ignored here, which limits the applicable interaction time.

The initial quantum states of experimental photonic pulses or BECs typically has a shot-to-shot randomness in the state preparation that results in experimental number fluctuations. It is common to have at least a Poissonian number variance [39] when the atom numbers are larger than 10^3. Accordingly, we assume Poissonian number fluctuations in the calculations given here, in order to represent typical initial quantum density matrices. The Wigner distribution $W[\psi]$ over Wigner fields ψ exists for any quantum state [36, 40]. It is not always positive definite. The usual operator time-evolution equation

$$\frac{d\hat{\psi}}{dt} = -i\left[\hat{H}, \hat{\psi}\right], \tag{5}$$

where the Hamiltonian $\hat{H}$ is defined by Eq. (3), can be transformed [41] into a differential equation for $W[\psi]$, typically with third or higher order derivatives. After truncation of third order derivatives [24], which are the highest order terms in a $1/N$ expansion for N particles, one obtains a second order Fokker-Plank equation for $W[\psi]$. This is an approximate functional differential equation for a probability distribution over Wigner fields.

When the evolution is unitary, this results in a partial differential equation for phase-space variables using well-known procedures [25, 26, 42]. The resulting equation for the Wigner field ψ, is:

$$\frac{d\psi}{dt} = i\nabla^2\psi - 2iC\psi\left(|\psi^2| - 1/\Delta z\right), \tag{6}$$

where Δz is the lattice spacing or inverse momentum cutoff. Quantum noise is present in the initial conditions. We start from a state with Poissonian number distribution, which is equivalent to a coherent state:

$$\hat{\rho}\,(t=0) = |\alpha\,(z)\rangle\langle\alpha\,(z)\,|, \tag{7}$$

where $|\alpha\,(z)\,|^2 = n\,(z)$. In the Wigner representation this is exactly represented by an ensemble of fields $\psi\,(z)$ with initial quantum noise η_k, with

$$\psi\,(z) = \sqrt{n\,(z)} + \frac{1}{\sqrt{2}}\sum_k \frac{1}{\sqrt{L}}\eta_k e^{ikz}. \tag{8}$$

Here η_k are complex random numbers correlated as $\langle\eta_k\eta^*_{k'}\rangle = \delta_{kk'}$, $\langle\eta_k\eta_{k'}\rangle = 0$. The functional integration over the Wigner distribution is performed by generating multiple random initial states and using them to seed independent integrations of the PDE. This results in a large number, N_s, of independent field modes — each evolving in time with equal probability.

The Wigner phase-space method generates a direct representation of symmetrically ordered quantum observables. To obtain the usual normally-ordered quantum observables, one must transform the results of a Wigner calculation from a symmetrically ordered to a normally ordered form. This also removes the divergence of symmetrically-ordered observables at large momentum cutoff. The expectation values of symmetrically ordered operator expressions can be obtained by integrating this equation over multiple independent trajectories to produce a set of values $\psi^{(j)}$ and averaging over a corresponding function of these values.

There is an approximate equality between symmetrically ordered quantum averages and Wigner averages,

where the N-dependent truncation error depends on the evaluated operator [43, 44]:

$$\left\langle \left\{ \hat{O}\left(\hat{\psi},\hat{\psi}^{\dagger}\right)\right\} \right\rangle \approx \left\langle \left\{ \hat{O}\right\} \right\rangle_{W} = \langle O\rangle_{W}. \tag{9}$$

We consider a quantum dynamical experiment where an initial state is prepared and then evolved in time. The initial state is a Poissonian mixture of uncorrelated particles with mean value $N = 10^3 - 10^4$ in a localized spatial mode. The equivalent coherent state has the classical soliton shape that occurs with some small initial coupling of $C_i = -2/N$, with r_0 as the characteristic initial size, so that in dimensionless units, $\alpha(z) = \sqrt{N/2}\,\mathrm{sech}(z)$.

This corresponds to an ultra-cold atomic Bose gas experiment, with a BEC initially trapped in a localized state with no interactions. At time $t = 0$, the interaction Hamiltonian is turned on to a larger value of $C_f = -8/N$, allowing particles to interact and forming a breather, a higher-order oscillating soliton. The resulting density profile, $\langle \hat{n}\,(z)\rangle = \left\langle \hat{\psi}^{\dagger}(z)\hat{\psi}(z)\right\rangle$, is shown in Fig. 1 for $N = 1000$ and in Fig. 2 for $N = 10000$. The result of the initial condition is that a high-order soliton or breather is formed [45], with a characteristic period of $\tau_b = \pi/4$. Our numerical results show characteristic breathing oscillations such that the mean breather amplitude decays with time.

This simulation is similar to related experimental proposals of first creating a fundamental soliton at weak coupling, then suddenly increasing the coupling strength. The coupling change would be caused by either a pulse entering a fiber in a photonic experiment, or else a change in a tunable Feshbach resonance in an atomic system. A number of different theoretical methods [22, 23, 28] have been used to analyze this type of proposed experiment, making it of topical interest. The present protocol employs a localized non-interacting BEC as the initial state, following earlier proposals [28, 29]. The timescales and numbers used are within the general parameter range achievable with current ^{7}Li [21] and ^{85}Rb [27] ultra-cold atomic physics experiments.

The simulation is sensitive to the selected spatial and momentum grids. The spatial grid must be symmetrical around 0 and have a point at $z = 0$, or else the decay happens on a faster scale, since there is insufficient lattice resolution for spatial convergence. The momentum grid should ideally be symmetrical around 0, which can be achieved by using a pair of position- and momentum-dependent coefficients applied before and after the Fourier transform. If this condition is not satisfied, the unbalanced high-momentum components of the noise lead to numerical errors. A finite lattice was used with periodic boundary conditions at $z = \pm L/2$. Results were obtained using a public domain stochastic partial differential equation code [46] with a fourth-order Runge-Kutta interaction picture algorithm [47],

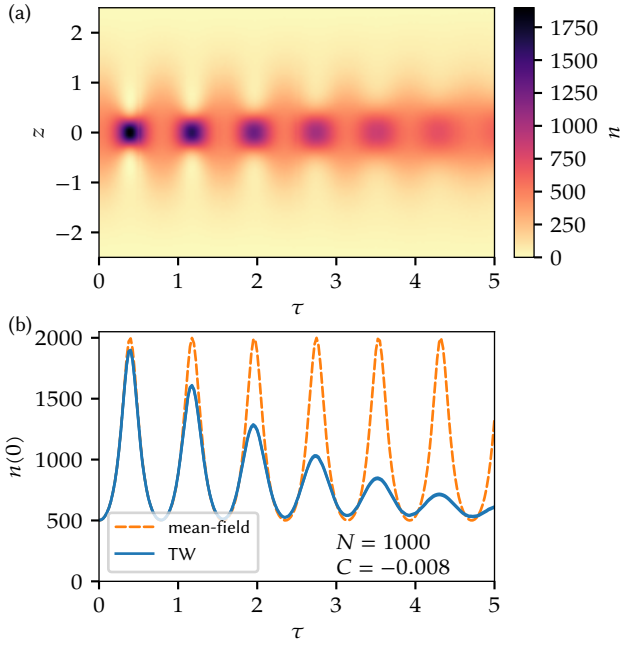

Figure 1. Density near the centre of the simulation area (a) and at $z = 0$ (b) over time. Simulation with $N = 10^3$, $C = -8 \times 10^{-3}$, $M = 512$, $L = 20$, 10^5 trajectories, 10^5 time steps. The area between the simulation curves (solid blue lines) denotes the estimated sampling error. The result of the mean-field simulation (dashed orange lines) are shown for comparison. The time-step errors are smaller than the line thickness and are not shown on the graph.

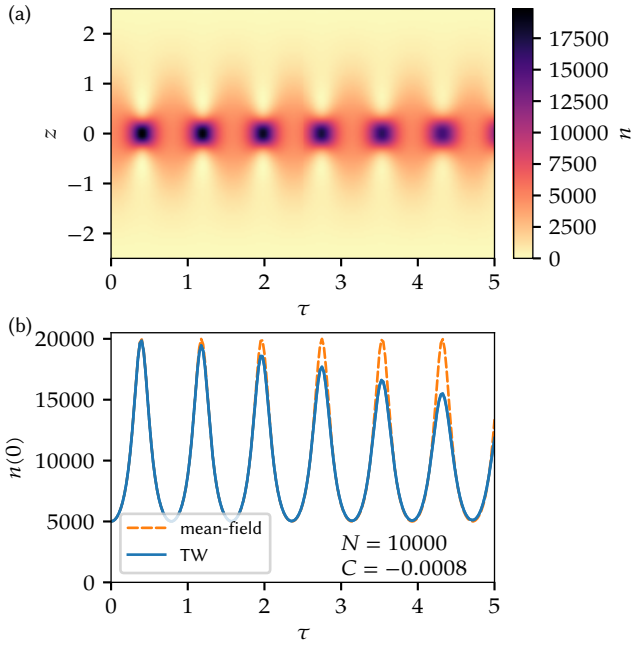

Figure 2. Density near the centre of the simulation area (a) and at $z = 0$ (b) over time. Simulation with $N = 10^4$, $C = -8 \times 10^{-4}$, other properties as in Fig. 1.

then cross-checked with a larger number of samples using an open source graphical processor unit (GPU) code.

The initial density matrix used here is a random phase mixture of coherent states. This is exactly equivalent to a Poissonian mixture of initial pure number states in a single spatial mode, chosen as $u = \mathrm{sech}\,(z)/\sqrt{2}$, similar to previous investigations [28, 29]. Since the measurements phase-independent, only a single phase in the mixture is calculated. Averaging over phases would produce identical results in every input phase.In the present examples, the initial boson number is $N_{\rm in} = N \pm \sqrt{N}$, where $N = 10^3 - 10^4$. The number standard deviation is $\pm\sqrt{N}$, or $\pm 1\% - 3.2\%$, which is typical for these types of experiment.

Convergence tests were carried out with the four exact conservation laws, $\hat{N}$, $\hat{P}$, $\hat{H}$, $\hat{H}_3$ [48], and with exact COM expansion predictions [49, 50]. All agreed with the predicted conserved behavior, apart from small errors of size $N^{-3/2}$ [30]. The comparison with these tests will be reported in detail elsewhere. Truncated Wigner methods can have a growing truncation error with time [51, 52]; however, earlier variational results were not able to satisfy these tests [29]. The main issue is whether the breather behaves classically, or whether the oscillations are damped owing to quantum fragmentation of the higher-order soliton. This problem is extremely challenging in quantum many-body theory, as it involves exponentially many eigenstates. As can be seen by the results given here, in the TW approximation the oscillations are predicted to decay gradually, without sudden fragmentation as predicted using variational methods [28].

Since the center-of mass position is known to spread, one may expect that the on-axis density plotted in Fig. 1 and Fig. 2 might decay purely due to the quantum uncertainty in the final position. Therefore, in Fig. 3, we introduce the dimensionless Glauber second order correlation function, $G^{(2)}(z_1, z_2) = \left\langle \hat{\psi}^\dagger(z_1)\,\hat{\psi}^\dagger(z_2)\,\hat{\psi}(z_2)\,\hat{\psi}(z_1)\right\rangle$, and investigate the integrated correlation:

$$\mu = \int G^{(2)}(z, z)\, dz/N^2. \tag{10}$$

This integrated correlation function measures the "peakedness" of a spatial distribution, in a way that is independent of the location of the peak. This also decays, although not as strongly as the on-axis density. We conclude that the breather appears to gradually radiate or fragment due to quantum effects with increasing similarity to mean field behaviour as $N \to \infty$. This is confirmed by an eigenvalue analysis of the first order correlation function, $G^{(1)}(z_1, z_2) = \left\langle \hat{\psi}^\dagger(z_1)\,\hat{\psi}(z_2)\right\rangle$. The definition of a Bose condensate is that it has a macroscopic occupation [53]of a single eigenmode of $G^{(1)}$. The transition to a partially fragmented BEC is illustrated in Fig. 4, which shows that six modes dynamically evolve to $> 1\%$ occupation by $\tau = 5$. This cannot be treated accurately by variational calculations with fewer modes [29].

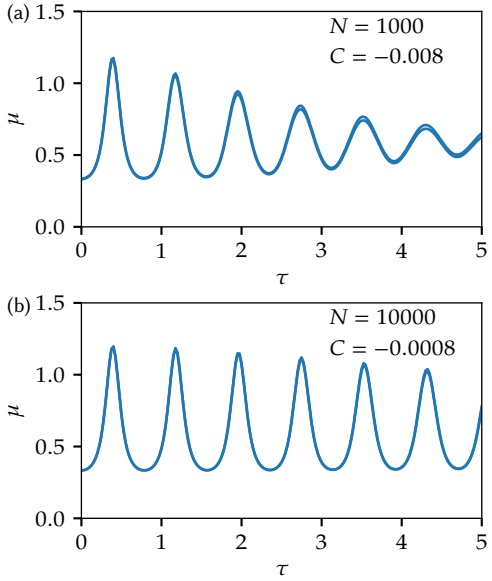

Figure 3. Correlation μ over time. Simulation with $N = 10^3$, $C = -8{\times}10^{-3}$ (a) and $N = 10^4$, $C = -8{\times}10^{-4}$ (b), $M = 512$, $L = 20$, 10^5 trajectories, 10^5 time steps. The area between the simulation curves (solid blue lines) denotes the estimated sampling error. The time-step errors are smaller than the line thickness and are not shown on the graph.

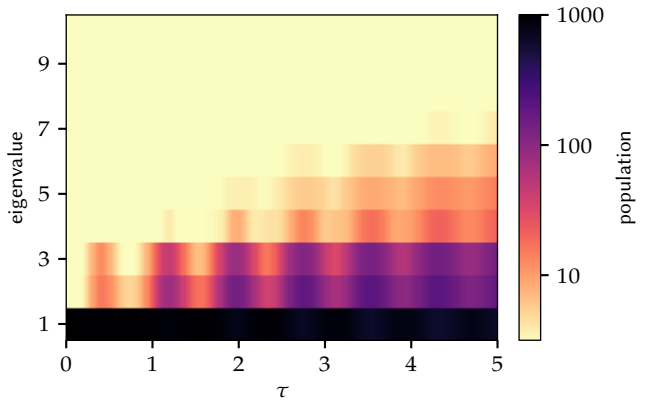

Figure 4. Eigenvalues of the correlation function $G^{(1)}$ over time. Simulation with $N = 10^3$, $C = -8 \times 10^{-3}$ $M = 512$, $L = 20$, 10^3 trajectories, 10^5 time steps. The graph shows increasing fragmentation with time.

In summary, our results predict continuous quantum fragmentation of higher-order soliton breathers at particle numbers of $N = 1000$, with results closer to mean field predictions at $N = 10000$. This is readily testable in BEC experiments.

We would like to acknowledge helpful discussions with J. Brand, J. Cosme, R. Hulet, B. Malomed, M. Olshanii and L. Carr. This work was performed in part at Aspen Center for Physics, which is supported by National

Science Foundation grant PHY-1607611.

[1] M. Rosenbluh and R. M. Shelby, Phys. Rev. Lett. **66**, 153 (1991).

[2] P. D. Drummond, R. M. Shelby, S. R. Friberg, and Y. Yamamoto, Nature **365**, 307 (1993).

[3] J. Heersink, V. Josse, G. Leuchs, and U. L. Andersen, Opt. Lett. **30**, 1192 (2005).

[4] J. F. Corney, P. D. Drummond, J. Heersink, V. Josse, G. Leuchs, and U. L. Andersen, Phys. Rev. Lett. **97**, 023606 (2006).

[5] H. B. Thacker, Reviews of Modern Physics **53**, 253 (1981).

[6] E. H. Lieb and W. Liniger, Physical Review **130**, 1605 (1963).

[7] J. B. McGuire, Journal of Mathematical Physics **5**, 622 (1964).

[8] D. M. Gangardt and G. V. Shlyapnikov, Phys. Rev. Lett. **90**, 010401 (2003).

[9] K. V. Kheruntsyan, D. M. Gangardt, P. D. Drummond, and G. V. Shlyapnikov, Physical review letters **91**, 040403 (2003).

[10] K. V. Kheruntsyan, D. M. Gangardt, P. D. Drummond, and G. V. Shlyapnikov, Physical Review A **71**, 053615 (2005).

[11] V. A. Yurovsky, M. Olshanii, and D. S. Weiss, Advances in Atomic, Molecular, and Optical Physics **55**, 61 (2008).

[12] B. Laburthe Tolra, K. M. O'Hara, J. H. Huckans, W. D. Phillips, S. L. Rolston, and J. V. Porto, Physical review letters **92**, 190401 (2004).

[13] T. Kinoshita, T. Wenger, and D. S. Weiss, Phys. Rev. Lett. **95**, 190406 (2005).

[14] T. Langen, S. Erne, R. Geiger, B. Rauer, T. Schweigler, M. Kuhnert, W. Rohringer, I. E. Mazets, T. Gasenzer, and J. Schmiedmayer, Science **348**, 207 (2015).

[15] M. Rigol, V. Dunjko, V. Yurovsky, and M. Olshanii, Physical review letters **98**, 050405 (2007).

[16] L. Khaykovich, F. Schreck, G. Ferrari, T. Bourdel, J. Cubizolles, L. D. Carr, Y. Castin, and C. Salomon, Science **296**, 1290 (2002).

[17] K. Strecker, G. Partridge, A. Truscott, and R. Hulet, Nature **417**, 150 (2002).

[18] P. Medley, M. A. Minar, N. C. Cizek, D. Berryrieser, and M. A. Kasevich, Physical review letters **112**, 060401 (2014).

[19] G. D. McDonald, C. C. N. Kuhn, K. S. Hardman, S. Bennetts, P. J. Everitt, P. A. Altin, J. E. Debs, J. D. Close, and N. P. Robins, Physical review letters **113**, 013002 (2014).

[20] J. H. Nguyen, P. Dyke, D. Luo, B. A. Malomed, and R. G. Hulet, arXiv preprint arXiv:1407.5087 (2014).

[21] J. H. Nguyen, D. Luo, and R. G. Hulet, Science **356**, 422 (2017).

[22] C. Weiss and L. D. Carr, arXiv preprint arXiv:1612.05545 (2016).

[23] V. A. Yurovsky, B. A. Malomed, R. G. Hulet, and M. Olshanii, arXiv preprint arXiv:1706.07114 (2017).

[24] R. Graham, *Quantum Statistics in Optics and Solid-State Physics*, edited by G. Hohler, Vol. 66 (Springer, New York, 1973) p. 1.

[25] P. D. Drummond and A. D. Hardman, Europhysics Letters (EPL) **21**, 279 (1993).

[26] M. J. Steel, M. K. Olsen, L. I. Plimak, P. D. Drummond, S. M. Tan, M. J. Collett, D. F. Walls, and R. Graham, Physical Review A **58**, 4824 (1998).

[27] P. Everitt, M. Sooriyabandara, M. Guasoni, P. Wigley, C. Wei, G. McDonald, K. Hardman, P. Manju, J. Close, C. Kuhn, *et al.*, Phys. Rev. A **96**, 041601(R) (2017).

[28] A. I. Streltsov, O. E. Alon, and L. S. Cederbaum, Physical review letters **100**, 130401 (2008).

[29] J. G. Cosme, C. Weiss, and J. Brand, Physical Review A **94**, 043603 (2016).

[30] P. D. Drummond and B. Opanchuk, accepted to Phys. Rev. A (2017).

[31] P. Drummond and S. Carter, JOSA B **4**, 1565 (1987).

[32] M. Olshanii, Physical Review Letters **81**, 938 (1998).

[33] S. J. Carter, P. D. Drummond, M. D. Reid, and R. M. Shelby, Phys. Rev. Lett. **58**, 1841 (1987).

[34] J. P. Gordon, Optics letters **11**, 662 (1986).

[35] S. J. Carter and P. D. Drummond, Physical review letters **67**, 3757 (1991).

[36] E. P. Wigner, Phys. Rev. **40**, 749 (1932).

[37] R. J. Glauber, Phys. Rev. **131**, 2766 (1963).

[38] J. F. Corney, J. Heersink, R. Dong, V. Josse, P. D. Drummond, G. Leuchs, and U. L. Andersen, Phys. Rev. A **78**, 023831 (2008).

[39] C.-S. Chuu, F. Schreck, T. P. Meyrath, J. L. Hanssen, G. N. Price, and M. G. Raizen, Physical review letters **95**, 260403 (2005).

[40] M. Hillery, R. F. O'Connell, M. O. Scully, and E. P. Wigner, Physics reports **106**, 121 (1984).

[41] J. Moyal, Proceedings of the Cambridge Philosophical Society **45**, 99 (1949).

[42] B. Opanchuk and P. D. Drummond, Journal of Mathematical Physics **54**, 042107 (2013).

[43] P. Kinsler, M. Fernée, and P. D. Drummond, Physical Review A **48**, 3310 (1993).

[44] P. Kinsler, Phys. Rev. A **53**, 2000 (1996).

[45] P. Wai, C. R. Menyuk, Y. Lee, and H. Chen, Optics letters **11**, 464 (1986).

[46] S. Kiesewetter, R. Polkinghorne, B. Opanchuk, and P. D. Drummond, SoftwareX **5**, 12 (2016).

[47] B. M. Caradoc-Davies, *Vortex dynamics in Bose-Einstein condensates*, Ph.D. thesis (2000).

[48] B. Davies, Physica A: Statistical Mechanics and its Applications **167**, 433 (1990).

[49] W. Kohn, Physical Review **123**, 1242 (1961).

[50] T. Vaughan, P. Drummond, and G. Leuchs, Physical Review A **75**, 033617 (2007).

[51] A. Sinatra, C. Lobo, and Y. Castin, Journal of Physics B: Atomic, Molecular and Optical Physics **35**, 3599 (2002), arXiv:condmat/0201217.

[52] P. P. Deuar and P. D. Drummond, Phys. Rev. Lett. **98**, 120402 (2007).

[53] O. Penrose and L. Onsager, Physical Review **104**, 576 (1956).